

Search for the decays $B_d^0 \rightarrow \mu^+ \mu^-$ and $B_s^0 \rightarrow \mu^+ \mu^-$ in $p\bar{p}$ collisions at $\sqrt{s} = 1.8$ TeV

- F. Abe,¹⁷ H. Akimoto,³⁹ A. Akopian,³¹ M. G. Albrow,⁷ A. Amadon,⁵ S. R. Amendolia,²⁷ D. Amidei,²⁰ J. Antos,³³
 S. Aota,³⁷ G. Apollinari,³¹ T. Arisawa,³⁹ T. Asakawa,³⁷ W. Ashmanskas,¹⁸ M. Atac,⁷ P. Azzi-Bacchetta,²⁵ N. Bacchetta,²⁵
 S. Bagdasarov,³¹ M. W. Bailey,²² P. de Barbaro,³⁰ A. Barbaro-Galtieri,¹⁸ V. E. Barnes,²⁹ B. A. Barnett,¹⁵ M. Barone,⁹
 G. Bauer,¹⁹ T. Baumann,¹¹ F. Bedeschi,²⁷ S. Behrends,³ S. Belforte,²⁷ G. Bellettini,²⁷ J. Bellinger,⁴⁰ D. Benjamin,³⁵
 J. Bensinger,³ A. Beretvas,⁷ J. P. Berge,⁷ J. Berryhill,⁵ S. Bertolucci,⁹ S. Bettelli,²⁷ B. Bevensee,²⁶ A. Bhatti,³¹
 K. Biery,⁷ C. Bigongiari,²⁷ M. Binkley,⁷ D. Bisello,²⁵ R. E. Blair,¹ C. Blocker,³ S. Blusk,³⁰ A. Bodek,³⁰ W. Bokhari,²⁶
 G. Bolla,²⁹ Y. Bonushkin,⁴ D. Bortoletto,²⁹ J. Boudreau,²⁸ L. Breccia,² C. Bromberg,²¹ N. Bruner,²² R. Brunetti,²
 E. Buckley-Geer,⁷ H. S. Budd,³⁰ K. Burkett,²⁰ G. Busetto,²⁵ A. Byon-Wagner,⁷ K. L. Byrum,¹ M. Campbell,²⁰
 A. Caner,²⁷ W. Carithers,¹⁸ D. Carlsmith,⁴⁰ J. Cassada,³⁰ A. Castro,²⁵ D. Cauz,³⁶ A. Cerri,²⁷ P. S. Chang,³³ P. T. Chang,³³
 H. Y. Chao,³³ J. Chapman,²⁰ M.-T. Cheng,³³ M. Chertok,³⁴ G. Chiarelli,²⁷ C. N. Chiou,³³ L. Christofek,¹³ M. L. Chu,³³
 S. Cihangir,⁷ A. G. Clark,¹⁰ M. Cobal,²⁷ E. Cocca,²⁷ M. Contreras,⁵ J. Conway,³² J. Cooper,⁷ M. Cordelli,⁹ D. Costanzo,²⁷
 C. Couyoumtzelis,¹⁰ D. Cronin-Hennessy,⁶ R. Culbertson,⁵ D. Dagenhart,³⁸ T. Daniels,¹⁹ F. DeJongh,⁷
 S. Dell'Agnello,⁹ M. Dell'Orso,²⁷ R. Demina,⁷ L. Demortier,³¹ M. Deninno,² P. F. Derwent,⁷ T. Devlin,³² J. R. Dittmann,⁶
 S. Donati,²⁷ J. Done,³⁴ T. Dorigo,²⁵ N. Eddy,²⁰ K. Einsweiler,¹⁸ J. E. Elias,⁷ R. Ely,¹⁸ E. Engels, Jr.,²⁸ W. Erdmann,⁷
 D. Errede,¹³ S. Errede,¹³ Q. Fan,³⁰ R. G. Feild,⁴¹ Z. Feng,¹⁵ C. Ferretti,²⁷ I. Fiori,² B. Flaugher,⁷ G. W. Foster,⁷ M. Franklin,¹¹
 J. Freeman,⁷ J. Friedman,¹⁹ Y. Fukui,¹⁷ S. Gadomski,¹⁴ S. Galeotti,²⁷ M. Gallinaro,²⁶ O. Ganel,³⁵ M. Garcia-Sciveres,¹⁸
 A. F. Garfinkel,²⁹ C. Gay,⁴¹ S. Geer,⁷ D. W. Gerdes,¹⁵ P. Giannetti,²⁷ N. Giokaris,³¹ P. Giromini,⁹ G. Giusti,²⁷ M. Gold,²²
 A. Gordon,¹¹ A. T. Goshaw,⁶ Y. Gotra,²⁵ K. Goulianios,³¹ H. Grassmann,³⁶ L. Groer,³² C. Grossi-Pilcher,⁵ G. Guillian,²⁰
 J. Guimaraes da Costa,¹⁵ R. S. Guo,³³ C. Haber,¹⁸ E. Hafen,¹⁹ S. R. Hahn,⁷ R. Hamilton,¹¹ T. Handa,¹² R. Handler,⁴⁰
 F. Happacher,⁹ K. Hara,³⁷ A. D. Hardman,²⁹ R. M. Harris,⁷ F. Hartmann,¹⁶ J. Hauser,⁴ E. Hayashi,³⁷ J. Heinrich,²⁶
 W. Hao,³⁵ B. Hinrichsen,¹⁴ K. D. Hoffman,²⁹ M. Hohlmann,⁵ C. Holck,²⁶ R. Hollebeek,²⁶ L. Holloway,¹³ Z. Huang,²⁰
 B. T. Huffman,²⁸ R. Hughes,²³ J. Huston,²¹ J. Huth,¹¹ H. Ikeda,³⁷ M. Incagli,²⁷ J. Incandela,⁷ G. Introzzi,²⁷ J. Iwai,³⁹
 Y. Iwata,¹² E. James,²⁰ H. Jensen,⁷ U. Joshi,⁷ E. Kajfasz,²⁵ H. Kambara,¹⁰ T. Kamon,³⁴ T. Kaneko,³⁷ K. Karr,³⁸ H. Kasha,⁴¹
 Y. Kato,²⁴ T. A. Keaffaber,²⁹ K. Kelley,¹⁹ R. D. Kennedy,⁷ R. Kephart,⁷ D. Kestenbaum,¹¹ D. Khazins,⁶ T. Kikuchi,³⁷
 B. J. Kim,²⁷ H. S. Kim,¹⁴ S. H. Kim,³⁷ Y. K. Kim,¹⁸ L. Kirsch,³ S. Klimentko,⁸ D. Knoblauch,¹⁶ P. Koehn,²³ A. Köngeter,¹⁶
 K. Kondo,³⁷ J. Konigsberg,⁸ K. Kordas,¹⁴ A. Korytov,⁸ E. Kovacs,¹ W. Kowald,⁶ J. Kroll,²⁶ M. Kruse,³⁰
 S. E. Kuhlmann,¹ E. Kuns,³² K. Kurino,¹² T. Kuwabara,³⁷ A. T. Laasanen,²⁹ I. Nakano,¹² S. Lami,²⁷ S. Lammel,⁷
 J. I. Lamoureux,³ M. Lancaster,¹⁸ M. Lanzoni,²⁷ G. Latino,²⁷ T. LeCompte,¹ S. Leone,²⁷ P. Limon,⁷ M. Lindgren,⁴
 T. M. Liss,¹³ J. B. Liu,³⁰ Y. C. Liu,³³ N. Lockyer,²⁶ O. Long,²⁶ C. Loomis,³² M. Loretti,²⁵ D. Lucchesi,²⁷ P. Lukens,⁷
 S. Lusin,⁴⁰ J. Lys,¹⁸ K. Maeshima,⁷ P. Maksimovic,¹⁹ M. Mangano,²⁷ M. Mariotti,²⁵ J. P. Marriner,⁷ A. Martin,⁴¹
 J. A. J. Matthews,²² P. Mazzanti,² P. McIntyre,³⁴ P. Melese,³¹ M. Menguzzato,²⁵ A. Menzione,²⁷ E. Meschi,²⁷
 S. Metzler,²⁶ C. Miao,²⁰ T. Miao,⁷ G. Michail,¹¹ R. Miller,²¹ H. Minato,³⁷ S. Miscetti,⁹ M. Mishina,¹⁷ S. Miyashita,³⁷
 N. Moggi,²⁷ E. Moore,²² Y. Morita,¹⁷ A. Mukherjee,⁷ T. Muller,¹⁶ P. Murat,²⁷ S. Murgia,²¹ H. Nakada,³⁷ I. Nakano,¹²
 C. Nelson,⁷ D. Neuberger,¹⁶ C. Newman-Holmes,⁷ C.-Y. P. Ngan,¹⁹ L. Nodulman,¹ S. H. Oh,⁶ T. Ohmoto,¹²
 T. Ohsugi,¹² R. Oishi,³⁷ M. Okabe,³⁷ T. Okusawa,²⁴ J. Olsen,⁴⁰ C. Pagliarone,²⁷ R. Paoletti,²⁷ V. Papadimitriou,³⁵
 S. P. Pappas,⁴¹ N. Parashar,²⁷ A. Parri,⁹ J. Patrick,⁷ G. Paulette,³⁶ M. Paulini,¹⁸ A. Perazzo,²⁷ L. Pescara,²⁵ M. D. Peters,¹⁸
 T. J. Phillips,⁶ G. Piacentino,²⁷ M. Pillai,³⁰ K. T. Pitts,⁷ R. Plunkett,⁷ L. Pondrom,⁴⁰ J. Proudfoot,¹ F. Ptahos,¹¹
 G. Punzi,²⁷ K. Ragan,¹⁴ D. Reher,¹⁸ M. Reischl,¹⁶ A. Ribon,²⁵ F. Rimondi,² L. Ristori,²⁷ W. J. Robertson,⁶ T. Rodrigo,²⁷
 S. Rolli,³⁸ L. Rosenson,¹⁹ R. Roser,¹³ T. Saab,¹⁴ W. K. Sakamoto,³⁰ D. Saltzberg,⁴ A. Sansoni,⁹ L. Santi,³⁶ H. Sato,³⁷
 P. Schlabach,⁷ E. E. Schmidt,⁷ M. P. Schmidt,⁴¹ A. Scott,⁴ A. Scribano,²⁷ S. Segler,⁷ S. Seidel,²² Y. Seiya,³⁷ F. Semeria,²
 T. Shah,¹⁹ M. D. Shapiro,¹⁸ N. M. Shaw,²⁹ P. F. Shepard,²⁸ T. Shibayama,³⁷ M. Shimojima,³⁷ M. Shochet,⁵
 J. Siegrist,¹⁸ A. Sill,³⁵ P. Sinervo,¹⁴ P. Singh,¹³ K. Sliwa,³⁸ C. Smith,¹⁵ F. D. Snider,¹⁵ J. Spalding,⁷ T. Speer,¹⁰ P. Sphicas,¹⁹
 F. Spinella,²⁷ M. Spiropulu,¹¹ L. Spiegel,⁷ L. Stanco,²⁵ J. Steele,⁴⁰ A. Stefanini,²⁷ R. Ströhmer,⁷ J. Strologas,¹³
 F. Strumia,¹⁰ D. Stuart,⁷ K. Sumorok,¹⁹ J. Suzuki,³⁷ T. Suzuki,³⁷ T. Takahashi,²⁴ T. Takano,²⁴ R. Takashima,¹² K. Takikawa,³⁷
 M. Tanaka,³⁷ B. Tannenbaum,²² F. Tartarelli,²⁷ W. Taylor,¹⁴ M. Tecchio,²⁰ P. K. Teng,³³ Y. Teramoto,²⁴ K. Terashi,³⁷
 S. Tether,¹⁹ D. Theriot,⁷ T. L. Thomas,²² R. Thurman-Keup,¹ M. Timko,³⁸ P. Tipton,³⁰ A. Titov,³¹ S. Tkaczyk,⁷ D. Toback,⁵
 K. Tollefson,¹⁹ A. Tollestrup,⁷ H. Toyoda,²⁴ W. Trischuk,¹⁴ J. F. de Troconiz,¹¹ S. Truitt,²⁰ J. Tseng,¹⁹ N. Turini,²⁷
 T. Uchida,³⁷ F. Ukegawa,²⁶ J. Valls,³² S. C. van den Brink,²⁸ S. Vejcik, III,²⁰ G. Velev,²⁷ R. Vidal,⁷ R. Vilar,⁷ D. Vucinic,¹⁹
 R. G. Wagner,¹ R. L. Wagner,⁷ J. Wahl,⁵ N. B. Wallace,²⁷ A. M. Walsh,³² C. Wang,⁶ C. H. Wang,³³ M. J. Wang,³³
 A. Warburton,¹⁴ T. Watanabe,³⁷ T. Watts,³² R. Webb,³⁴ C. Wei,⁶ H. Wenzel,¹⁶ W. C. Wester, III,⁷ A. B. Wicklund,¹
 E. Wicklund,⁷ R. Wilkinson,²⁶ H. H. Williams,²⁶ P. Wilson,⁵ B. L. Winer,²³ D. Winn,²⁰ D. Wolinski,²⁰ J. Wolinski,²¹
 S. Worm,²² X. Wu,¹⁰ J. Wyss,²⁷ A. Yagil,⁷ W. Yao,¹⁸ K. Yasuoka,³⁷ G. P. Yeh,⁷ P. Yeh,³³ J. Yoh,⁷ C. Yosef,²¹ T. Yoshida,²⁴
 I. Yu,⁷ A. Zanetti,³⁶ F. Zetti,²⁷ and S. Zucchelli²

(CDF Collaboration)

- ¹Argonne National Laboratory, Argonne, Illinois 60439
²Istituto Nazionale di Fisica Nucleare, University of Bologna, I-40127 Bologna, Italy
³Brandeis University, Waltham, Massachusetts 02254
⁴University of California at Los Angeles, Los Angeles, California 90024
⁵University of Chicago, Chicago, Illinois 60637
⁶Duke University, Durham, North Carolina 27708
⁷Fermi National Accelerator Laboratory, Batavia, Illinois 60510
⁸University of Florida, Gainesville, Florida 32611
⁹Laboratori Nazionali di Frascati, Istituto Nazionale di Fisica Nucleare, I-00044 Frascati, Italy
¹⁰University of Geneva, CH-1211 Geneva 4, Switzerland
¹¹Harvard University, Cambridge, Massachusetts 02138
¹²Hiroshima University, Higashi-Hiroshima 724, Japan
¹³University of Illinois, Urbana, Illinois 61801
¹⁴Institute of Particle Physics, McGill University, Montreal H3A 2T8,
and University of Toronto, Toronto M5S 1A7, Canada
¹⁵The Johns Hopkins University, Baltimore, Maryland 21218
¹⁶Institut für Experimentelle Kernphysik, Universität Karlsruhe, 76128 Karlsruhe, Germany
¹⁷National Laboratory for High Energy Physics (KEK), Tsukuba, Ibaraki 305, Japan
¹⁸Ernest Orlando Lawrence Berkeley National Laboratory, Berkeley, California 94720
¹⁹Massachusetts Institute of Technology, Cambridge, Massachusetts 02139
²⁰University of Michigan, Ann Arbor, Michigan 48109
²¹Michigan State University, East Lansing, Michigan 48824
²²University of New Mexico, Albuquerque, New Mexico 87131
²³The Ohio State University, Columbus, Ohio 43210
²⁴Osaka City University, Osaka 588, Japan
²⁵Università di Padova, Istituto Nazionale di Fisica Nucleare, Sezione di Padova, I-35131 Padova, Italy
²⁶University of Pennsylvania, Philadelphia, Pennsylvania 19104
²⁷Istituto Nazionale di Fisica Nucleare, University and Scuola Normale Superiore of Pisa, I-56100 Pisa, Italy
²⁸University of Pittsburgh, Pittsburgh, Pennsylvania 15260
²⁹Purdue University, West Lafayette, Indiana 47907
³⁰University of Rochester, Rochester, New York 14627
³¹Rockefeller University, New York, New York 10021
³²Rutgers University, Piscataway, New Jersey 08855
³³Academia Sinica, Taipei, Taiwan 11530, Republic of China
³⁴Texas A&M University, College Station, Texas 77843
³⁵Texas Tech University, Lubbock, Texas 79409
³⁶Istituto Nazionale di Fisica Nucleare, University of Trieste/Udine, Italy
³⁷University of Tsukuba, Tsukuba, Ibaraki 315, Japan
³⁸Tufts University, Medford, Massachusetts 02155
³⁹Waseda University, Tokyo 169, Japan
⁴⁰University of Wisconsin, Madison, Wisconsin 53706
⁴¹Yale University, New Haven, Connecticut 06520

(Received 21 November 1997; published 27 February 1998)

We present a search for the flavor-changing neutral current decays $B_d^0 \rightarrow \mu^+ \mu^-$ and $B_s^0 \rightarrow \mu^+ \mu^-$ in $p\bar{p}$ collisions at $\sqrt{s}=1.8$ TeV, using 98 pb^{-1} of data collected at the Collider Detector at Fermilab. We find one candidate event for these decays, which is consistent with the background estimates, and set upper limits on the branching fractions of $\mathcal{B}(B_d^0 \rightarrow \mu^+ \mu^-) < 8.6 \times 10^{-7}$ and $\mathcal{B}(B_s^0 \rightarrow \mu^+ \mu^-) < 2.6 \times 10^{-6}$ at 95% confidence level. [S0556-2821(98)50207-X]

PACS number(s): 14.40.Nd, 13.20.He

In the standard model of electroweak interactions, the decays $B^0 \rightarrow \mu^+ \mu^-$ [1] are forbidden for tree level processes. However they can proceed at a low rate through higher order flavor-changing neutral current (FCNC) processes. Theory [2] predicts branching fractions of $(1.5 \pm 0.9) \times 10^{-10}$ and $(3.5 \pm 1.0) \times 10^{-9}$ for $B_d^0 \rightarrow \mu^+ \mu^-$ and $B_s^0 \rightarrow \mu^+ \mu^-$ decays, respectively. Higher branching fractions would indicate contributions from physics beyond the standard model. Our previous measurement [3], using $17.8 \pm 0.6 \text{ pb}^{-1}$ of $p\bar{p}$ data

collected during the 1992–1993 running period (Run 1A), obtained $\mathcal{B}(B_d^0 \rightarrow \mu^+ \mu^-) < 1.6 \times 10^{-6}$ and $\mathcal{B}(B_s^0 \rightarrow \mu^+ \mu^-) < 8.4 \times 10^{-6}$ at 90% C.L. These are more stringent limits than obtained at the Y(4S) (B_d^0 only) [4], Z^0 [5] or at other $p\bar{p}$ collider experiments [6]. An additional $80.4 \pm 6.4 \text{ pb}^{-1}$ of data has been collected during the 1994–1995 running period (Run 1B). In this paper we use the combined data set of $98 \pm 6.4 \text{ pb}^{-1}$. This result supersedes our previous work.

The Collider Detector at Fermilab (CDF) has been de-

scribed in detail elsewhere [7]. The detector components most relevant to this measurement are the tracking system and the muon chambers. The tracking system, which is immersed in a 1.4 T solenoidal magnetic field, consists of three detector systems. The innermost tracking device is a silicon micro-strip vertex detector (SVX) [8] which provides spatial measurements in the $r\text{-}\phi$ [9] plane. The SVX consists of two identical cylindrical barrels and has an active region of 51 cm in z . Each barrel consists of four layers of silicon strip detectors with 60 μm pitch between readout strips for the three inner layers and 55 μm pitch for the fourth layer. The layers are located at radii between 3.0 and 7.9 cm from the beam line. The impact parameter resolution of the SVX is $\sigma_D(p_T) = (13 + 40/p_T) \mu\text{m}$ where p_T is the transverse momentum of the track in GeV/c . The track impact parameter D is defined as the distance of closest approach, measured in the plane perpendicular to the beam, of the track helix to the beam axis.

The SVX is followed by a set of time projection chambers (VTX) which measure the position of the proton-antiproton interaction position (the primary vertex) along the beam line. Surrounding the VTX is the central tracking chamber (CTC), a 3 m long cylindrical drift chamber ranging from 0.3 to 1.3 m in radius covering the pseudorapidity interval $|\eta| < 1.0$. The CTC contains 84 layers of sense wires, grouped into nine alternating axial and stereo super layers.

The central muon system, consisting of three components (CMU, CMP, and CMX), is capable of detecting muons with $p_T \geq 1.4 \text{ GeV}/c$ in the pseudorapidity interval $|\eta| < 1.0$. The CMU system covers the region $|\eta| < 0.6$ and consists of 4 layers of planar drift chambers outside the hadron calorimeter allowing the reconstruction of track segments for charged particles penetrating the 5 absorption lengths of material. Outside the CMU there are 3 additional absorption lengths of steel followed by 4 layers of drift chambers (CMP). Finally, the CMX system extends the coverage up to pseudorapidity $|\eta| < 1.0$. Depending on the incident angle, particles have to penetrate 6–9 absorption lengths of material to be detected in the CMX. For the Run 1A selection, only the CMU was used.

CDF has a three level trigger system. The first two levels are implemented in hardware, while the third is a software trigger which is a version of the offline reconstruction software optimized for speed. The Level 1 triggers relevant for this analysis require two track segments in the muon chambers. At Level 2, tracks found in the CTC by the central fast track processor (CFT) [10] are associated to track segments in the muon chambers. Two different p_T thresholds are used in our trigger, depending on whether one or both muons are required to be found in the CFT. When one muon is associated to a CFT track, the CFT algorithm is 50% efficient for tracks with $p_T = 2.6 \text{ GeV}/c$, and this efficiency rises to 96% for tracks with $p_T > 3.1 \text{ GeV}/c$. Triggers containing two matches between the CFT and muon track segments are 50% efficient for tracks with $p_T = 1.95 \text{ GeV}/c$, and reach the plateau at $2.3 \text{ GeV}/c$. The Level 3 trigger requires two muon candidates after full reconstruction. During Run 1B, Level 3 required at least one of the two muons to be detected in the CMP. During Run 1A CMX muons were not included in the dimuon triggers.

The following muon selection criteria are applied: the separation between the track in the muon chamber and the

extrapolated CTC track is calculated in both the transverse and longitudinal planes. In each view, the difference is required to be less than 3.0 standard deviations (σ) from zero, where σ is the sum in quadrature of the multiple scattering and measurement uncertainties. The energy deposited in the hadronic calorimeter by each muon is required to be greater than 0.5 GeV, which is σ lower (where σ is the standard deviation which is calculated using the Landau distribution below the peak) than the average expected energy loss from a minimum ionizing particle. The p_T of each muon is required to be greater than $2 \text{ GeV}/c$. The p_T of the muon pair is required to be greater than $6 \text{ GeV}/c$ in order to be able to normalize our result with our previously measured B_d^0 production cross section [11]. The invariant mass of the muon pair is derived from a vertex fit of the two muon tracks where the tracks are constrained to come from a common vertex. Candidates failing the fit procedure are discarded.

The long lifetime of B mesons permits us to use the proper decay length as a strong rejection criteria against short-lived background. This requires a precise measurement of the position of the B meson decay (the decay vertex) and the distance the B meson traveled before decaying (the decay length). For this reason, both muons are required to be reconstructed in the SVX, with hits in at least 3 of the 4 layers. The uncertainty on the transverse decay length, $L_{xy} = \vec{l}_{xy} \cdot \vec{p}_T(\mu^+ \mu^-)/p_T(\mu^+ \mu^-)$, is required to be $< 150 \mu\text{m}$, where \vec{l}_{xy} is the vector pointing from the primary vertex (the interaction point) to the secondary vertex (the reconstructed decay position) and $\vec{p}_T(\mu^+ \mu^-)$ is the transverse momentum vector of the muon pair determined using quantities derived in the vertex fit described above. The mean uncertainty of L_{xy} is $\approx 60 \mu\text{m}$, which is significantly smaller than the mean transverse decay length of $\approx 860 \mu\text{m}$ expected for the signal.

The following selection criteria are applied to select candidate B mesons. The proper decay length, $\lambda = L_{xy} \times [m_{B^0}/p_T(\mu^+ \mu^-)]$, is required to be greater than $100 \mu\text{m}$. This requirement reduces the number of muon pairs with opposite charge (OS) in the $5\text{--}6 \text{ GeV}/c^2$ mass range from 4095 to 729.

Due to the hard b fragmentation [12], B mesons carry most of the transverse momentum of the b -quark. We require the isolation of the muon pair, defined as $I = p_T(\mu^+ \mu^-)/[p_T(\mu^+ \mu^-) + \sum p_T]$, to be greater than 0.75. The sum is the scalar sum of the transverse momenta of all the tracks, except the two candidate muons, within a cone of $\Delta R = 1$ [$\Delta R = \sqrt{(\Delta \eta)^2 + (\Delta \phi)^2}$] around the momentum vector of the muon pair. The z coordinate of these tracks must be within 5 cm of the B candidate vertex to exclude tracks from other $p\bar{p}$ collisions that can occur during the same bunch crossing. The isolation requirement reduces the number of OS muon pairs to 80.

The vectors $\vec{p}_T(\mu^+ \mu^-)$ and \vec{l}_{xy} are required to point in the same direction, the opening angle Φ (pointing angle) between $\vec{p}_T(\mu^+ \mu^-)$ and \vec{l}_{xy} is required to be less than 0.1 radians. Figure 1 shows the distribution of the pointing angle for the Monte Carlo prediction (see below) and the like sign (LS) muon pair data. LS muon pairs are used as an estimate of the pointing angle distribution of the background. This

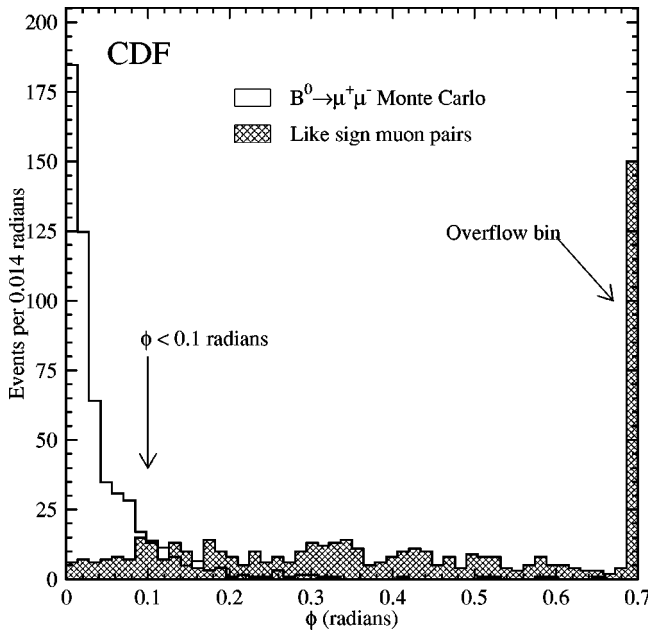


FIG. 1. Distribution of the pointing angle [the angle between $\vec{p}_T(\mu^+\mu^-)$ and \vec{l}_{xy}] for Monte Carlo and like sign (LS) muon pairs in the 5 to 6 GeV/c^2 mass range after all selection criteria, except the pointing angle and isolation requirement have been applied. LS muon pairs are used as an estimate of the isolation distribution of background events. The arrow indicates the chosen cut.

requirement reduces the number of OS (LS) muon pairs in the 5–6 GeV/c^2 mass range to 5 (6), respectively.

The proper decay length, isolation and pointing requirements have been optimized by maximizing the signal-to-background significance, $\epsilon_{\text{Sig}}^2/\epsilon_{\text{Bgr}}$, where ϵ_{Sig} is the efficiency for $B^0 \rightarrow \mu^+\mu^-$ events, and ϵ_{Bgr} is the efficiency for background events. To estimate ϵ_{Bgr} we use LS muon pairs

in the 5–6 GeV/c^2 mass range as a sample of pure background.

Table I lists the acceptance and the efficiency for each of the selection criteria. In this analysis, several different triggers were used during different running periods. Each trigger has a corresponding efficiency and acceptance for each period. The quoted efficiencies of Table I are weighted according to luminosity and trigger contribution in each run period.

The acceptance, as well as the efficiencies of $\sigma(L_{xy})$, and muon- p_T selection criteria have been estimated by Monte Carlo simulation. We generate b quarks according to a next-to-leading order QCD calculation [13] with minimum b -quark $p_T > 5.5 \text{ GeV}/c$ and $|y(b)| < 1.3$, then fragment them into B mesons using the Peterson *et al.* parametrization [12] with $\epsilon_b = 0.006$. The B mesons are then forced to decay into $\mu^+\mu^-$ and the resulting muons are subjected to a full simulation of the CDF detector and trigger.

The efficiency of the $\lambda > 100 \mu\text{m}$ requirement has been estimated by the same Monte Carlo simulation as above. The efficiencies of the isolation and pointing requirements were obtained using a sample of fully reconstructed $B^+ \rightarrow J/\psi K^+$ and $B^0 \rightarrow J/\psi K^{*0}$ events [14]. The uncertainty is determined by the statistics of the exclusive B sample. We assume the same efficiency of the isolation requirement for B_s^0 mesons. Figure 2 shows the distribution of the isolation variable for the background subtracted $J/\psi K^+$ and $J/\psi K^{*0}$ sample and the LS muon pair data. The efficiency of the pointing requirement was checked with the $B^0 \rightarrow \mu^+\mu^-$ Monte Carlo simulation and was found to agree well. The efficiency of the $\lambda > 100 \mu\text{m}$ requirement was checked with the exclusive B^0 and B^+ samples and was found to agree well with the Monte Carlo simulation. Using the Monte Carlo simulation, as well as extrapolating the mass resolution measured in the decays $J/\psi \rightarrow \mu^+\mu^-$, $\psi(2S) \rightarrow \mu^+\mu^-$, and $\Upsilon(1S) \rightarrow \mu^+\mu^-$, we estimate the mass resolution for $B^0 \rightarrow \mu^+\mu^-$ to be

TABLE I. List of efficiencies and their uncertainties (both statistical and systematic uncertainties are added in quadrature). The efficiencies are for B mesons with $p_T(B) > 6 \text{ GeV}/c$ and rapidity $|y(B)| < 1$. The total efficiency is the product of the individual efficiencies when applied in that order.

Cut	Efficiency in %
Geometrical acceptance for $p_T(B) > 6 \text{ GeV}/c$ and rapidity $ y(B) < 1$	10.72 ± 0.06
$p_T(\mu) > 2 \text{ GeV}/c$	89.6 ± 0.2
Dimuon triggers	58.3 ± 3.4
Track finding efficiency in the muon chambers	96.6 ± 0.7
Efficiency to reconstruct both μ tracks in the CTC offline	89.8 ± 3.6
Muon selection criteria	97.2 ± 1.2
Track and vertex quality selection criteria	77.1 ± 0.2
Uncertainty on the decay length ($\sigma_{L_{xy}} < 150 \mu\text{m}$)	94.7 ± 0.5
Decay length ($\lambda > 100 \mu\text{m}$)	80.9 ± 1.0 81.8 ± 1.6
Pointing angle: $\Phi < 0.1$	85.1 ± 2.2
Isolation: $I > 0.75$	72.8 ± 3.0
J/ψ -yield correction	84.6 ± 3.8
B meson search window	91.6 ± 4.0
Total efficiency \times acceptance	$\begin{cases} \text{for } B_d \\ \text{for } B_s \end{cases}$
	1.34 ± 0.15
	1.37 ± 0.15

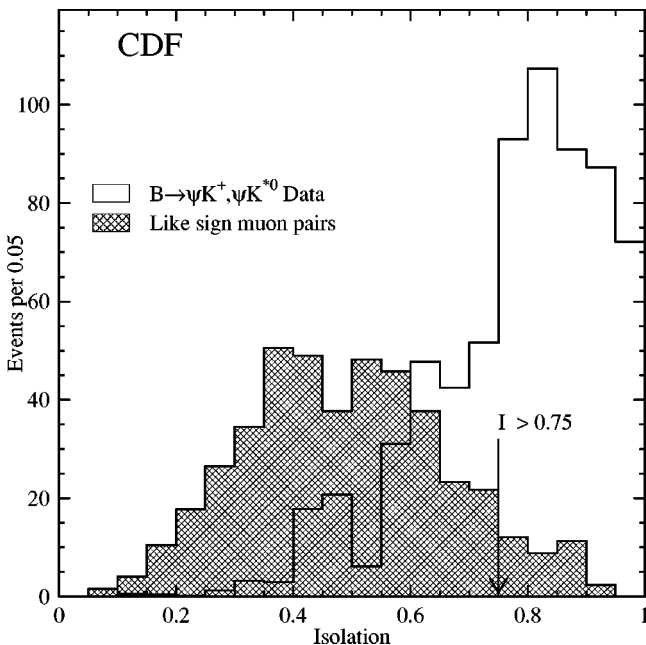


FIG. 2. Distribution of the isolation of background subtracted $J/\psi K^+$ and $J/\psi K^{*0}$ candidates and of like sign (LS) muon pairs in the 5 to 6 GeV/c^2 mass range after all selection criteria, except the pointing angle and isolation selection criteria. LS muon pairs are used as an estimate of the isolation distribution of background events. The arrow represents the chosen cut.

35 MeV/c^2 . For our search, we regard OS events passing all selection criteria as signal if they fall in the dimuon invariant mass regions 5.205–5.355 GeV/c^2 for the B_d^0 and 5.295–5.445 GeV/c^2 for the B_s^0 . The current world averages are: $m(B_d^0) = 5279.2 \pm 1.8 \text{ MeV}/c^2$ and $m(B_s^0) = 5369.3 \pm 2.0 \text{ MeV}/c^2$ [15]. Varying the mass resolution by $\pm 5 \text{ MeV}/c^2$ results in a 4% variation in the efficiency of the search window selection.

The muon matching requirement and dimuon trigger efficiencies have been estimated using a large J/ψ sample. The tracking efficiency has been estimated by embedding two Monte Carlo generated tracks into real data J/ψ events. After all efficiency corrections have been applied, the observed J/ψ yield in Run 1B is still found to be 18.8 ± 4.6 (stat.) % lower than the yield in Run 1A. This discrepancy in yield remains under investigation. For this analysis, an additional normalization correction has been imposed to the Run 1B data to make the J/ψ yield constant over the entire data set, and consistent with the data used in our B -production cross section measurement. The yield is taken as the number of long-lived ($\lambda > 100 \mu\text{m}$) J/ψ from the decay of B -hadrons corrected for tracking and trigger efficiency as well as acceptance and luminosity. The total efficiency and acceptance is $1.34 \pm 0.15\%$ for B_d^0 and $1.37 \pm 0.15\%$ for B_s^0 , including both statistical and systematic uncertainties.

The invariant mass distribution of the muon pairs passing all the selection criteria is shown in Fig. 3. One OS event with an invariant mass of $5.344 \pm 0.016 \text{ GeV}/c^2$ remains in the signal region. As it is in the overlapping part of the search windows, this will give one candidate for both B_d^0 and B_s^0 . The observed event is consistent with the background estimates from the LS muon pairs and from sideband events

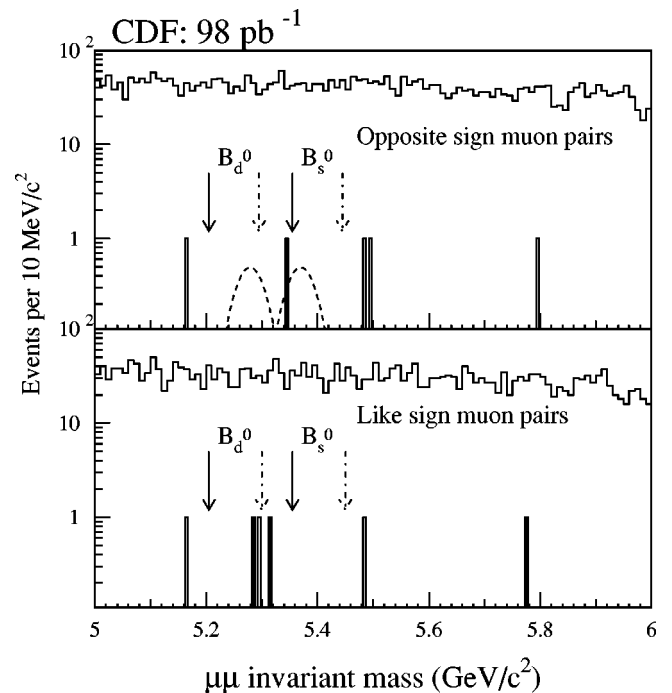


FIG. 3. Invariant mass distribution of like sign (LS) and opposite sign (OS) muon pairs before (higher histogram) and after (lower histogram) the proper decay time, isolation, and pointing angle criteria. The two plotted functions represent the 90% C.L. upper limit with the expected resolution and including the systematic uncertainty. The areas under the curves correspond to 4.31 events at 90% C.L. The $B_d^0(B_s^0)$ meson search windows are indicated by the solid(dashed) arrows. LS muon pairs are used as an estimate of the background.

(in the 5.0–5.2 GeV/c^2 and 5.5–6.0 GeV/c^2 mass ranges). To be conservative the upper limit of candidates allowed at 90% C.L., N_{limit} , is calculated assuming that the one event is a signal event. This results in a Poisson upper limit of 3.89 events at 90% C.L. The upper limit on the branching fractions is calculated from the formula

$$\mathcal{B}(B^0 \rightarrow \mu^+ \mu^-) < \frac{N_{limit}(B^0 \text{ or } \bar{B}^0 \rightarrow \mu^+ \mu^-)}{2 \cdot \sigma(B) \cdot \sum_i \int \mathcal{L}_i dt \cdot \epsilon_i \cdot \alpha_i},$$

where Σ_i represents the sum over all triggers and data samples contributing to the sample. The total integrated luminosity is given by $\int \mathcal{L}_i dt$, ϵ_i is the selection efficiency and α_i is the geometrical acceptance. CDF has measured the B_d^0 integrated production cross section for $p_T(B) > 6 \text{ GeV}/c$ and rapidity $|y(B)| < 1$ to be $\sigma(B_d^0) = 2.39 \pm 0.32 \pm 0.44 \mu\text{b}$ [11]. We assume $\sigma(B_d^0)/\sigma(B_s^0) = 1/3$ which is consistent with our measurement [16]. We do not use the measured value for the cross section ratio, as it depends on other assumptions. As the B^0 and \bar{B}^0 are not distinguished, a factor of 2 must be included.

The systematic uncertainties are listed in Table II. To include them in our limit calculation we use the procedure described in Ref. [17]. The systematic uncertainties due to the B production and decay kinematics are already included in the systematic uncertainty of the B production cross section. When including the systematic uncertainty, the upper

TABLE II. List of systematic uncertainties.

Source of systematic uncertainty	Fractional uncertainty in %
B meson cross section	22.6
Integrated luminosity	6.7
Efficiency \times acceptance	11.0
Total	26.0

limit of candidates is 4.31(5.48) at 90(95)% C.L., respectively. We obtain the following 90% and 95% C.L. upper limits:

$$\mathcal{B}(B_d^0 \rightarrow \mu^+ \mu^-) < 6.8 \times 10^{-7} \text{ (90% C.L.)}$$

$$\mathcal{B}(B_s^0 \rightarrow \mu^+ \mu^-) < 2.0 \times 10^{-6} \text{ (90% C.L.)}$$

and

$$\mathcal{B}(B_d^0 \rightarrow \mu^+ \mu^-) < 8.6 \times 10^{-7} \text{ (95% C.L.)}$$

$$\mathcal{B}(B_s^0 \rightarrow \mu^+ \mu^-) < 2.6 \times 10^{-6} \text{ (95% C.L.)}.$$

Compared to the previous analysis [3], two changes to the selection criteria are introduced: the isolation requirement is modified and the pointing angle Φ requirement is added. While the candidate found in the previous analysis does not pass the pointing angle criteria, one new candidate is found in the Run 1B data. In conclusion, we have observed no significant signal for FCNC decays of B mesons into dimuons. The resulting limits are a significant improvement over the previously published results, but still orders of magnitude away from the standard model prediction.

We thank the Fermilab staff and the technical staffs of the participating institutions for their vital contributions. This work was supported by the U.S. Department of Energy and National Science Foundation; the Italian Istituto Nazionale di Fisica Nucleare; the Ministry of Education, Science and Culture of Japan; the Natural Sciences and Engineering Research Council of Canada; the National Science Council of the Republic of China; the A. P. Sloan Foundation; and the Swiss National Science Foundation.

-
- [1] Although the official name of the B_d^0 is B^0 , we will use in this paper the first notation when referring to it. When referring to the decay $B^0 \rightarrow \mu^+ \mu^-$, we refer to both decays $B_d^0 \rightarrow \mu^+ \mu^-$ and $B_s^0 \rightarrow \mu^+ \mu^-$, and the charge conjugation is implied.
- [2] A. Ali, C. Greub, and T. Mannel, in *Proceedings of the ECFA Workshop on the Physics of the European B Meson Factory, 1993*, edited by R. Aleksan and A. Ali, p. 155; A. Ali, Report No. DESY 97-019, hep-ph/9702312, “Flavour Changing Neutral Current Processes in B Decays,” 1997.
- [3] CDF Collaboration, F. Abe *et al.*, Phys. Rev. Lett. **76**, 4675 (1996).
- [4] CLEO Collaboration, R. Ammar *et al.*, Phys. Rev. D **49**, 5701 (1994); ARGUS Collaboration, K. Albrecht *et al.*, Phys. Lett. B **199**, 451 (1987).
- [5] L3 Collaboration, M. Acciarri *et al.*, Phys. Lett. B **391**, 474 (1997).
- [6] UA1 Collaboration, C. Albajar *et al.*, Phys. Lett. B **262**, 163 (1991).
- [7] CDF Collaboration, F. Abe *et al.*, Nucl. Instrum. Methods Phys. Res. A **271**, 387 (1988); CDF Collaboration, F. Abe *et al.*, Phys. Rev. D **50**, 2966 (1994).
- [8] D. Amidei *et al.*, Nucl. Instrum. Methods Phys. Res. A **350**, 73 (1994).
- [9] The polar angle (θ) in cylindrical coordinates is measured from the proton beam which defines the z -axis, and the azimuthal angle (ϕ) from the plane of the Fermilab Tevatron. The rapidity (y) is defined as $y = \tanh^{-1}(p_z/E)$. The pseudorapidity (η) is defined as $\eta = -\ln[\tan(\theta/2)]$. Throughout this paper “transverse” refers to the plane perpendicular to the proton beam and “longitudinal” refers to the axis parallel to the proton beam (z -axis).
- [10] G. Foster *et al.*, Nucl. Instrum. Methods Phys. Res. A **269**, 93 (1988).
- [11] CDF Collaboration, F. Abe *et al.*, Phys. Rev. Lett. **75**, 1451 (1995).
- [12] C. Peterson *et al.*, Phys. Rev. D **27**, 105 (1983).
- [13] P. Nason, S. Dawson, and R. Ellis, Nucl. Phys. **B326**, 49 (1988); P. Dawson *et al.*, *ibid.* **B327**, 49 (1988); M. Mangano *et al.*, *ibid.* **B373**, 295 (1992).
- [14] F. Abe *et al.*, Report No. FERMILAB-PUB-97/352-E.
- [15] Particle Data Group, R. M. Barnett *et al.*, Phys. Rev. D **54**, 1 (1996).
- [16] CDF Collaboration, F. Abe *et al.*, Phys. Rev. D **54**, 6596 (1996).
- [17] R. D. Cousins and V. L. Highland, Nucl. Instrum. Methods Phys. Res. A **320**, 331 (1992).